2011년 2월

석사학위논문

A Study on LOCA Diagnostics Using Artificial Intelligence Methods

조 선 대 학 교 대 학 원

원 자 력 공 학 과

이 성 한

A Study on LOCA Diagnostics Using Artificial Intelligence Methods

- 인공지능 방법을 이용한
LOCA 진단에 관한 연구 -

2011년 2월 25일

조 선 대 학 교 대 학 원

원 자 력 공 학 과

이 성 한

A Study on LOCA Diagnostics Using Artificial Intelligence Methods

지도교수 나 만 균

이 논문을 공학 석사학위신청 논문으로 제출함.

2010년 10월

조 선 대 학 교 대 학 원

원 자 력 공 학 과

이 성 한

이성한의 석사학위 논문을 인준함

위원장　조선대학교　교수　송 종 순　(인)

위　원　조선대학교　교수　나 만 균　(인)

위　원　조선대학교 부교수 김 진 원　(인)

2010년　11월

조 선 대 학 교 대 학 원

CONTENTS

List of Tables

List of Figures

Abstract

A Study on LOCA Diagnostics Using Artificial Intelligence Methods

이 성 한

지도 교수 : 나 만 균

조선대학교 일반대학원 원자력공학과

원자력발전소에서 과도현상 혹은 사고가 발생시, 중대사고 관리전략을 효율적으로 달성하기 위하여 사건 초기의 아주 짧은 기간 동안 주요한 파라메타를 관측함으로써 초기사건을 파악하는 것이 중요하다. 본 논문에서는 원전 사고 시 초기조건 진단 방안으로 인공지능 방법론의 적용 가능성을 평가하고, 이를 이용한 중대사고 초기조건 진단체제를 개발하기 위하여 수행되었다. 이에 따라 다양한 인공지능 방법 (Group Method of Data Handling, Support Vector Machine)을 이용한 방법론을 검토하였으며, 이들 인공지능 방법론 중에 Support Vector Classification (SVC) 방법과 GMDH 및 Support Vector Regression (SVR) 방법을 이용하여 LOCA 사고의 위치를 알아내고, LOCA 파손 크기를 예측하는데 적용하였다.

고온관 LOCA 및 저온관 LOCA, 그리고 SGTR의 각 사고 유형에 대해 각각 111개씩 총 333개의 MAAP4 코드 사고 시뮬레이션 데이터를 이용하였으며, 선택된 입력 변수와 최대 예측 오차 및 RMS 오차, 측정 오차의 존재 및 SIS 작동에 의한 인공지능 방법의 성능을 분석한 결과, SVC는 모든 경우에 대하여 파열 위치를 정확하게 분류하였으며, GMDH와 SVR 모델은 정확한 파손 크기를 예측할 수 있었다. 대부분의 안전계통은 원자로 정지 후 보통 60초 이상의 지연을 가지고 작동하기 시작하므로, 본 논문에서는 원자로 정지 후 60초 이내에 적분된 신호를 입력 값으로 이용하였다. 또한, APR1400 원전에서 안전주입계통, 보조급수계통, 격납용기 살수계통의 작동 시간은 각각 40초, 60초, 80초이기 때문에 안전주입계통의 작동 효과만 고찰되었다.

Ⅰ. Introduction

If an accident occurs in a nuclear power plant, the plant operators might be provided with only partial information or not have sufficient time to analyze the accident in the urgent situation even though they are provided with enough information. In the beginning of the accident, plant operators will attempt to analyze the abnormal plant states by observing the temporal trends of a few important parameters. However, it is very difficult for operators to predict the progression of an accident by observing these temporal trends on large display panels in the main control room. During an accident, the operators will be faced with hundreds of instrument readings and alarms that will show some typical patterns of that accident. That is, accident management can be accomplished successfully from the operators' high level knowledge on what the initiating events are and where they have occurred. This knowledge can be obtained from important information obtained from a variety of measured data. The knowledge can be learned from the mining of important information from a variety of measured data. Therefore, it is expected that artificial intelligence methods equipped with learning systems can be applied to the accident management. In addition, many studies have examined accident management including event identification using artificial intelligence methods [1]-[4]. As a means of effectively managing severe accidents at nuclear plants, it is important to identify and diagnose the accident initiating events during an initial short time interval after the accidents by observing the major measured signals. Therefore, the accurate prediction of initiating events such as loss of coolant accident (LOCA), total loss of feed water (TLOFW), station blackout (SBO), steam generator tube rupture (SGTR) and major plant scenarios for severe accidents is required to manage the severe accidents. In the case a LOCA occurs in a nuclear power plant, it is important for the operators and technical staff to discover the location and size of the break by observing the

initial short time trends of the major parameters in order to develop a LOCA accident management strategy. Therefore, the break location should be discovered and the break size should be estimated accurately in order to provide operators and technical support personnel with the important and valuable information to successfully manage this type of accidents.

The objective of this thesis is to develop and verify the diagnostic techniques for LOCAs using artificial intelligence methods such as the SVC (support vector classification), GMDH (group method of data handling) and SVR (support vector regression) models. The inputs to the SVC, GMDH and SVR models are the time-integrated values of the important measured signals during a short time interval after a reactor scram. The proposed algorithm was verified using the simulation data of the MAAP4 code [5] for the advanced power reactor 1400 (APR1400), which is an advanced pressurized water reactor developed by the Korea Hydro & Nuclear Power company (KHNP).

Ⅱ. Recent Researches on Severe Accident Management

A severe accident is an accident that exceeds design-based accidents and results in core damage. When severe accidents are occurred at nuclear power plants, it is very difficult for operators to predict the progression of an accident because nuclear plant operators are provided with only partial information during the accident or they may have insufficient time to analyze the data despite being provided with considerable information. The accident management strategy is to give the operators and technical staff appropriate inputs to develop, follow and perform the corrective actions. The event identification can be classified as a pattern recognition problem.

Recently, among a variety of artificial intelligence methods, artificial neural networks were commonly used for severe accident management in order to identify accident scenarios [6] and develop symptom based diagnostic system [7] and nuclear power plant transient diagnosis [8]. An artificial neural network (ANN), usually called neural network (NN), is a mathematical model or computational model that is inspired by the way the biological neural networks. Neural networks can find non-linear descriptions from the input space into the output space, or they can find dependencies between several variables. A neural network consists of simple processing units called neurons. Generally, a neural network has three layers namely, the input, output and the hidden layers. The neurons in the input layer receive input from the external environment. This layer does not perform any computations. Hidden layer, which receives inputs from the input layer, performs computation and provides the outputs to the output layer. Output layer consists of neurons that communicate the output of the system to the user or external environment. The structure of a three-layer neural network is shown in Fig. 1. In most cases an ANN is an adaptive system that changes its structure based on

external or internal information that flows through the network during the learning phase. Modern neural networks are non-linear statistical data modeling tools. They are usually used to model complex relationships between inputs and outputs or to find patterns in data.

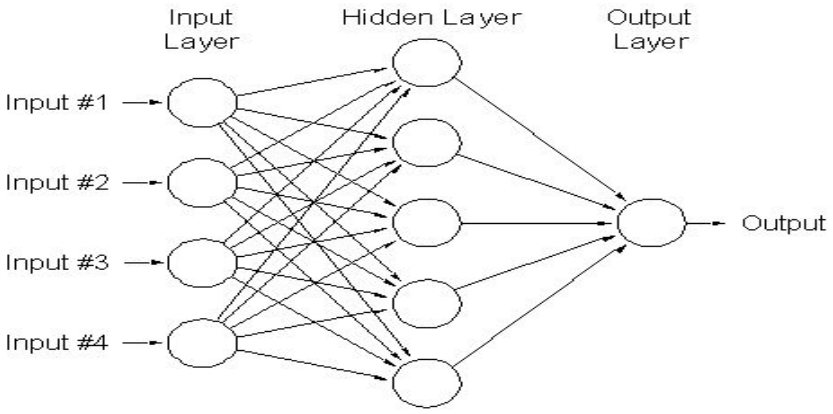

Fig. 1. Structure of a three-layer artificial neural network.

In particular, an operator support system, known as symptom based diagnostic system (SBDS), has been developed using artificial neural network that diagnoses the transients based on reactor process parameters, and continuously displays the status of the reactor. This will help the operator in identifying the event in advance and enables the operator to know the status of the plant at any instant of time during reactor operations. Whenever an event is detected, the system will display the important operator actions in addition to the type of initiating event and its time of occurrence [8].

Ⅲ. Artificial Intelligence Methods for LOCA Diagnostics

A. Identification of the Break Location

A general multi-class classification can be extended from a binary classification. To classify the data vectors into one of two classes based on a training data set, whose classification is known a priori, binary classification problems are given N training data $T=\{(\boldsymbol{x}_i,y_i)\}_{i=1}^{N}$, where $x_i\in R^m$ is the sample data vector y_i and indicates a class $y_i\in\{+1,-1\}$, from which an input-output relationship is learned. Each data vector x_i belongs to a class by $y_i\in\{+1,-1\}$.

In the case that two classes can be divided linearly, the data classification is accomplished by defining a hyperplane which divides the training data set T so that all the training data points of the same class are on the same side of the hyperplane while maximizing the distance between the hyperplane and the data point nearest the hyperplane. Fig. 2 gives an example of the classification for two-dimensional data vector using the SVC (Support vector Classification) model [9]. The hyperplane which bisects two classes can be expressed as follows:

$$w \cdot x + b = 0 \tag{1}$$

where the coefficient vector w and bias b determine the hyperplane.

The distance between the two parallel lines of $w \cdot x + b = 1$ and $w \cdot x + b = -1$ is $2/|w|$ as shown in Fig. 2. Accordingly, $w^T w$ should be minimized to maximize the distance between the two parallel lines. The generalized optimal separating hyperplane is determined by minimizing the following functional as follows:

$$\Phi(w,\xi) = \frac{1}{2}|w|^2 + \lambda\sum_{i=1}^{N}\xi_i \tag{2}$$

subject to the constraints

$$\begin{cases} y_i(w^T\phi(x)+b) \geq 1-\xi_i, & i=1,2,\cdots,N \\ \xi_i \geq 0, & i=1,2,\cdots,N \end{cases} \tag{3}$$

where

$$w = [w_1 \;\; w_2 \;\; \cdots \;\; w_N]^T$$

$$\xi = [\xi_1 \;\; \xi_2 \;\; \cdots \;\; \xi_N]^T.$$

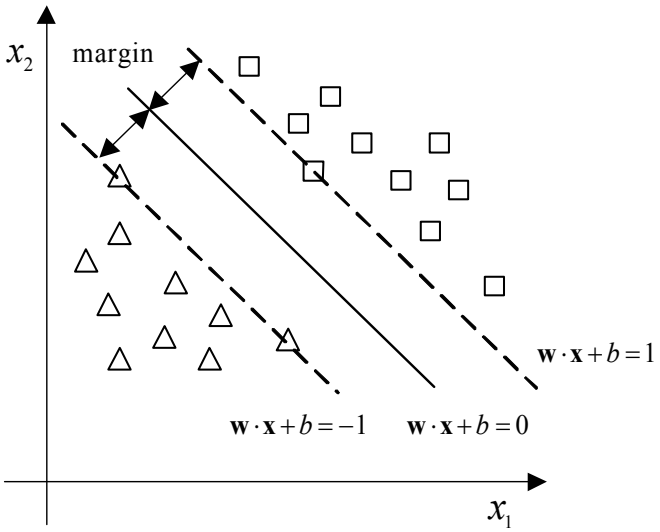

Fig. 2. An example of a binary classification using the SVC model [4][9].

The non-negative parameter ξ_i in the second term of Eq. (2) was used to deal with the problems related to a misclassification due to the noise on the data. In Fig. 3. the filled triangle and rectangle indicate the data with measurement noise. The parameter ξ_i is a measure of the misclassification.

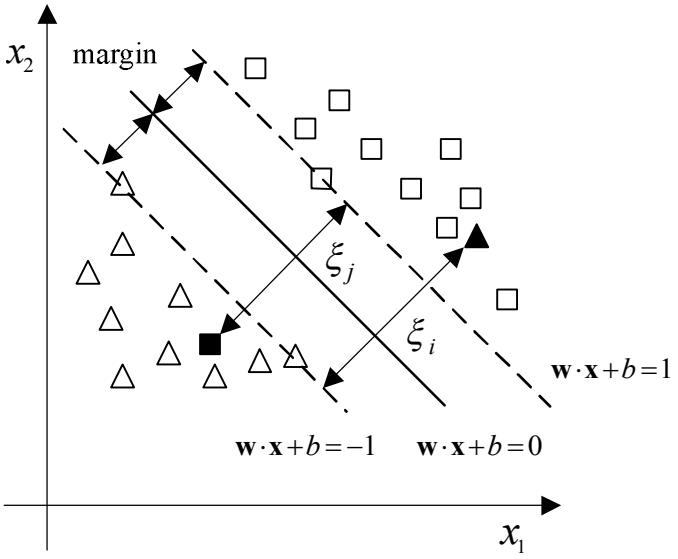

Fig. 3. An example of a misclassification due to noise in the measured data.

In the case where the linear boundary in the input spaces cannot separate the two classes properly, it is possible to create a hyperplane that allows a linear separation in higher dimensional feature space. The SVC models carry out this task by implicitly mapping the training data into higher dimensional feature space. A hyperplane is then constructed in this feature space that bisects the two categories and maximizes the margin of separation between itself and those points lying closest to it. Specifically, the primal space is transformed into high dimensional feature space by a nonlinear map $\phi(x)$, as shown in Fig. 4. The function, $\phi_i(x)$, is called the feature that is nonlinearly mapped from the input space x, and $\phi = [\phi_1 \ \phi_2 \ \cdots \ \phi_N]^T$. Fig. 4 shows the hyperplane established in high dimensional feature space and the nonlinear classification is replaced by a linear classification problem in high dimensional feature space. The parameter, λ, in Eq. (2) controls the trade-off between the complexity of the SVC model and the number of non-separable points, and is referred to as a regularization parameter.

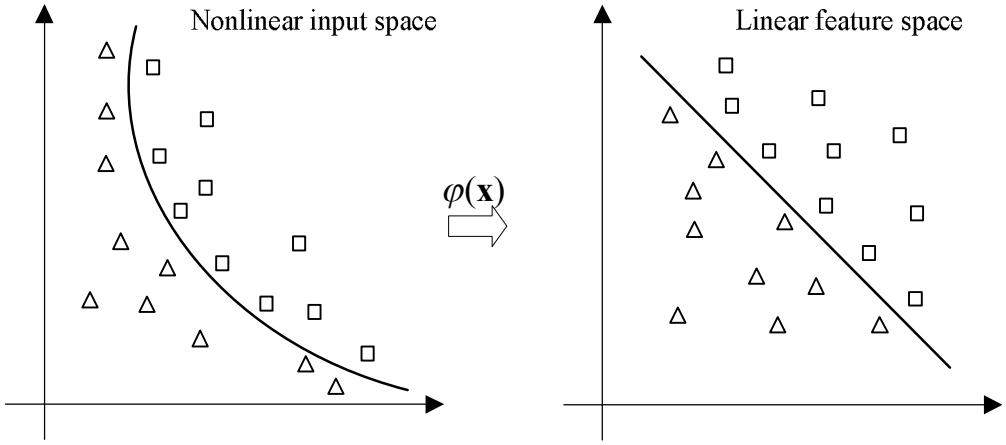

Fig. 4. Mapping to linear feature space from nonlinear input space [4].

The Lagrange multiplier technique and standard quadratic optimization technique can be used to solve the vector w and the bias b, and the solution to the convex optimization problem can be expressed as follows:

$$f(x) = sgn\left(\sum_{i \in SVs} \alpha_i y_i K(x_i, x) + b\right) \tag{4}$$

where $b^* = -\frac{1}{2}\sum_{i=1}^{N} \alpha_i y_i [K(x_i, x_r) + K(x_i, x_s)]$ is a bias term and $K(x_i, x) = \phi^T(x_i)\phi(x)$ is called the kernel function. In this thesis, a radial basis function, $K(x_i, x) = \exp\left(-\frac{(x - x_i)^T (x - x_i)}{2\sigma^2}\right)$, was used because the radial basis function showed the best performance in the simulation applications of this study.

In this thesis, the SVC models were used as a non-linear pattern classifier that identify the major LOCA break locations representing the hot-leg, cold-leg, and steam generator tubes (SGTs) observing some selected signals during a very short time immediately after a reactor scram. The input variables to the SVC models consist of the measured signals from the reactor coolant system, steam generators and containment at a nuclear power plant. These measured signals have information on the break locations, such as the hot-leg, cold-leg, and SGTs.

B. Estimation of Break Size

1. Group Method of Data Handling (GMDH) Method

A GMDH method was developed for the accurate estimation of the break size for LOCAs. Generally, the GMDH algorithm can automatically find interrelations in the data and select the optimal structure of the model. This method uses a data structure similar to that of multiple regression models. The data set can be divided into the training data set, checking data set and test data set. The reason for dividing the data set is to prevent over-fitting and maintain model parsimony. Fig. 5 shows the data structure used in the GMDH method with N being the number of observations and m the number of model inputs.

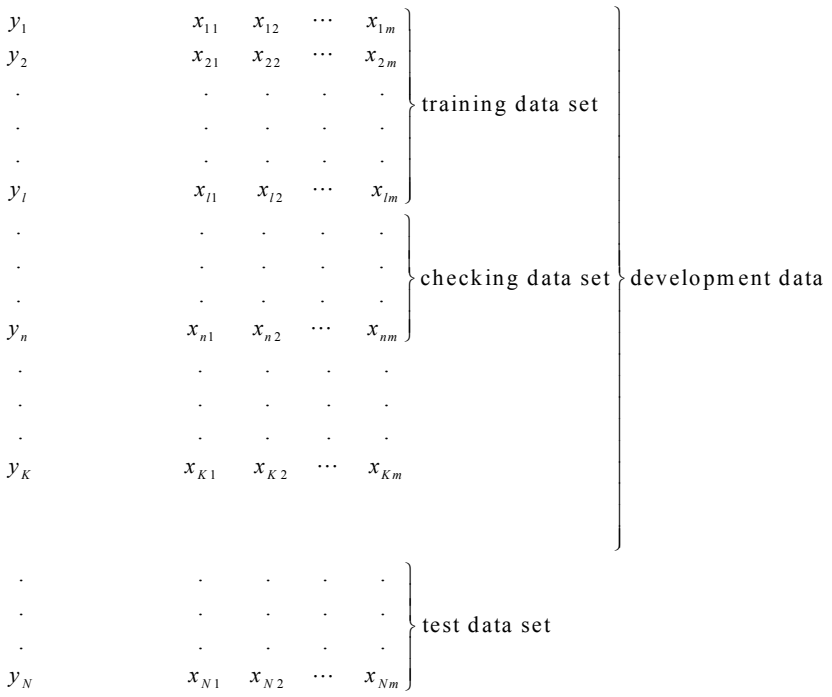

Fig. 5. GMDH data structure.

The GMDH uses a self-organizing modeling algorithm that can flexibly choose nonlinear forms of the basic inputs $\{x_1, x_2, \cdots, x_m\}$. Fig. 6 shows the branch structure of the GMDH algorithm [10]. It starts with the basic inputs at the first level and becomes more complex according to the increasing number of layers.

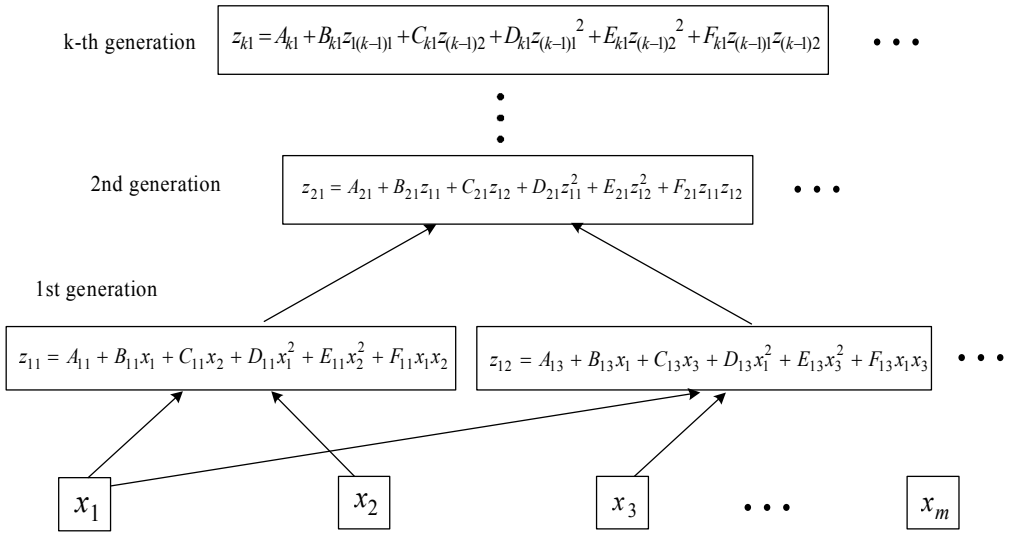

Fig. 6. Branch structure of the GMDH model [10].

The original GMDH method uses the following general form at each level of the successive approximation [10]-[12]:

$$y = f(x_i, x_j) = A + Bx_i + Cx_j + Dx_i^2 + Ex_j^2 + Fx_ix_j. \quad (5)$$

The coefficients of the above reference function, such as $A, B, \cdots F$, can be solved using a least squares method in an arbitrary pair (x_i, x_j) among independent variables $x = (x_1, x_2, \cdots, x_m)$. Although only quadratic terms are shown in Eq. (5), more complex functional forms, such as trigonometric terms ($\sin(c_1x)$ and $\cos(c_1x)$) and exponential terms ($\exp(-c_2x)$), can also be incorporated as input terms according to the complexity of the system.

The GMDH algorithm constructs a high-order polynomial of the

Kolmogorov-Gabor form:

$$y = a_0 + \sum_{i=1}^{m} a_i x_i + \sum_{i=1}^{m}\sum_{j=1}^{m} a_{ij} x_i x_j + \sum_{i=1}^{m} y \sum_{j=1}^{m}\sum_{k=1}^{m} a_{ijk} x_i x_j x_k \cdots \quad (6)$$

where $x = (x_1, x_2, \cdots, x_m)$ is an input variable vector and $a = (a_0, a_i, a_{ij}, a_{ijk}, \cdots)$ is a vector of coefficients or a weight of the Kolmogorov-Gabor polynomial.

The GMDH algorithm amalgamates lower order regression type polynomials at each generation to reach the next generation. This employs the composition of the lower order polynomials mentioned above (refer to Fig. 6). This process continues until the GMDH model begins to simulate the noise in training or it exceeds maximum calculation time (refer to Fig. 7).

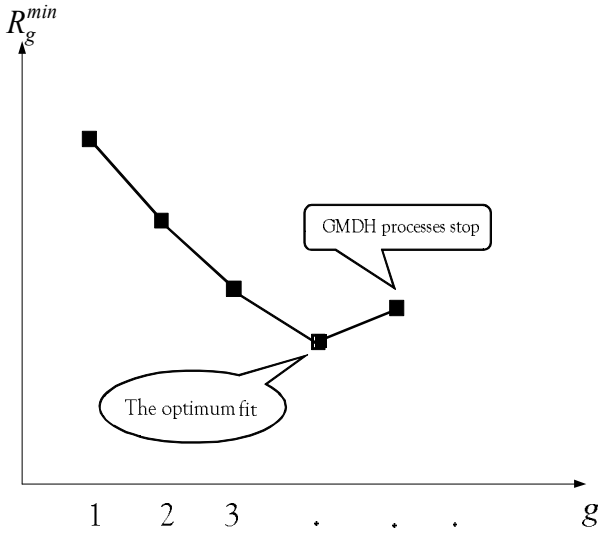

Fig. 7. Trend of the Rmin values according to the generations [10].

The GMDH algorithm has been developed and improved in many applications. The main steps in its implementation are as follows [10]:

1) Construct the input and corresponding output data for the GMDH model and divide them into training and checking data sets and normalize the data sets.

2) Choose the external inputs to the lowest level of the GMDH network. Calculate

the regression polynomial coefficients for each pair of input variables (x_i, x_j) and the associated output y in the training set. The linear regression coefficients are calculated using the least-squares method. Compute the $m(m-1)/2$ high-order variables in place of the original input variables $x_1, x_2, \cdots, x_m$ to estimate the output y. Ridge regression can also be applied to avoid the collinearity problem in solving the coefficient vector.

3) The algorithm has constructed a group of new variables $z_{g1}, z_{g2}, \cdots, z_{gm_g}$ $((m_g = m_{g-1}(m_{g-1}-1)/2)$) in the former step, where m_g is the number of input variables for generation g. Each of these new variables is evaluated by determining which variable best estimates the dependent variable y. The measure used to evaluate the new variables at each generation is the following fractional error for checking data:

$$r_j^2 = \frac{\sum_{i=l+1}^{n} (y_i - z_{ij})^2}{\sum_{i=l+1}^{n} y_i^2} \quad \text{for } j = 1, 2, \cdots, m_g. \tag{7}$$

where j is the number of layers. The columns of the new variable z_g are sorted in increasing order of r_j . An arbitrary cut-off R value is selected by the analyst. All columns of z_g satisfying $r_j < R$ are chosen to replace the input terms in the next layer, and all variables with $r_j > R$ are screened out and not passed onto the next generation of the algorithm (refer to Fig. 7).

4) The process above is performed repeatedly until over-fitting is found through cross checking. The minimum r_j value for generation g is denoted as $R_g^{\min}$. The training and checking processes stops if $R_g^{\min} > R_{g-1}^{\min}$. The polynomial with the minimum error criterion in generation $g-1$ is selected as the final approximate model. Otherwise, the algorithm moves to the next layer and repeats the above step (3) (refer to Fig. 7).

Fig. 7 shows that $R_g^{\min}$ has a quadratic shape [10] and GMDH converges to a

minimum value. Accordingly, as the generation proceeds from the bottom to the top in Fig. 6, the branch structure of the GMDH model becomes more complex and the empirical error of the GMDH model for a training data decreases continuously.

Compared to the training data, the empirical error of the GMDH model for checking data tends to decrease at an early stage with increasing generations but the error for the checking data begins to increase as the GMDH model becomes increasingly complex. Even if the error for a training data set is small, the GMDH model is overfitted if the error for a checking data begins to increase. At the end of the GMDH algorithm, all quadratic regression parameters are stored, and the estimated coefficients for the high order polynomial are determined by back tracing the GMDH architecture until the original variables $x_1, x_2, \cdots, x_m$ are reached. In addition, the change in the generations that generate the optimum fit can be expressed as a type of tree called an Ivakhnenko Tree (see Fig. 8).

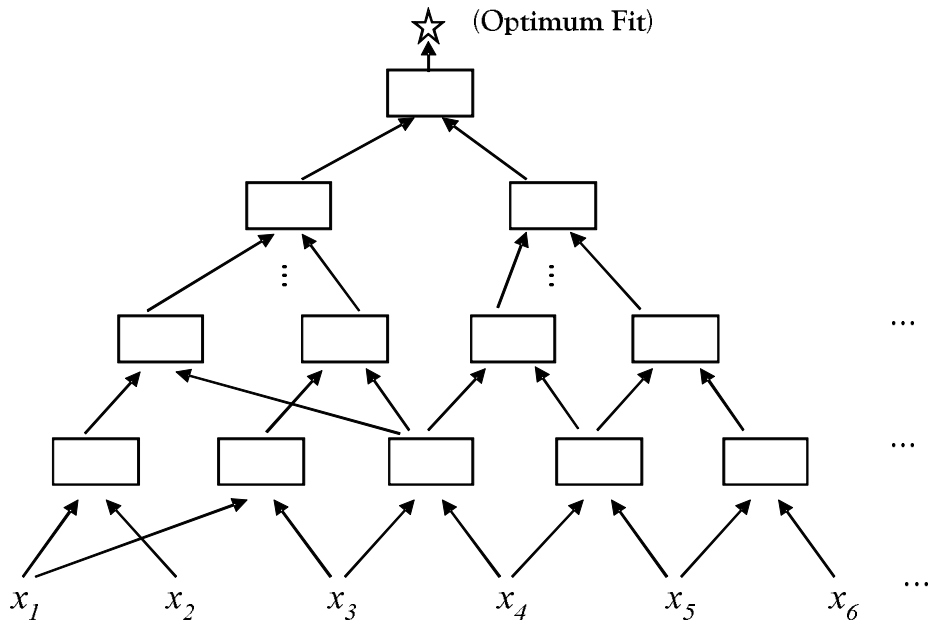

Fig. 8. Ivakhnenko tree.

Eq. (5) for a given data set (not one data point) is generally expressed as X^TX, where the coefficient vector W includes $A, B, \cdots F$. There are several problems in solving the coefficient vector W. Among them, collinearity is a problem frequently encountered during complex system modeling. A set of variables is collinear if there are one or more linear relationships between the variables. The problem of collinearity arises when there is a strong correlation between two or more independent variables. In this case, the coefficient estimates may change erratically in response to small changes in the data. In particular, the pseudo inverse calculation of a matrix including the column vectors with a strong correlation between them may induce a numerical stability problem. In this thesis, ridge regression was used to solve the collinearity problem. If we use a general least squares method, the coefficient vector is $W=(X^TX)^{-1}X^TY$. Since the calculation of $(X^TX)^{-1}$ may induce a numerical problem, the coefficient vector W was calculated from the ridge regression of the following form:

$$W=(X^TX+\alpha I)^{-1}X^TY, \tag{8}$$

where (X^TX) is the correlation matrix for the predictors, (X^TY) is the vector of the correlations between the predictors and the dependent variable, $\alpha \geq 0$ is a scalar constant (in this thesis, $\alpha = 10^{-6}$), and I is the identity matrix.

In this thesis, trigonometric terms ($\sin(c_1x)$ and $\cos(c_1x)$) and exponential terms ($\exp(-c_2x)$) were used in the reference function of Eq. (5). The constants c_1 and c_2 should be optimized. In addition, many measured signals are screened out from the measured input signals to the GMDH model by observing the graphical plots of the input and output (LOCA break size) signals at many data points as well as by analyzing the relationship between the input and output signals by calculating the covariance matrix of measured signals including the input and output signals. In addition, to optimize the GMDH model, optimization of the constants c_1 and c_2 and the final selection of the input signals were performed using a genetic algorithm.

Compared to the conventional optimization methods that move from one point to another, genetic algorithms start from many points simultaneously climbing many peaks in parallel. Accordingly, genetic algorithms are less susceptible to being trapped at local minima than conventional search methods [13]-[14]. Also, the genetic algorithm is the most useful method for solving optimization problems with multiple objectives. However, because the genetic algorithm requires much computational time if there are many parameters involved, we can combine the genetic algorithm with a least squares method to reduce the number of parameters that need to be optimized by the genetic algorithm. In genetic algorithms, the term chromosome refers to a candidate solution that minimizes a cost function, generally encoded as a bit string. As the generation proceeds, populations of chromosomes are iteratively altered by biological mechanisms inspired by natural evolution such as selection, crossover, and mutation. The genetic algorithms require a fitness function that assigns a score to each chromosome (candidate solution) in the current population, and maximize the fitness function value. In this thesis, a fitness function is suggested as follows:

$$F = \exp(-\mu_1 E_1 - \mu_2 E_2) \tag{9}$$

where μ_1 and μ_2 are the weighting coefficients, and E_1 and E_2 are defined as follows:

$$E_1 = \sqrt{\frac{1}{n}\sum_{k=1}^{n}(y_k - \hat{y_k})^2} \tag{10}$$

$$E_2 = m - 2 \tag{11}$$

where y_k and $\hat{y_k}$ denote the target and estimated values, respectively. n is the total number of training and verification data and n is the number of input signals. E_1 is presented to minimize root mean square (RMS) error and E_2 is used to maintain the number of input signals as small as possible.

2. Support Vector Regression (SVR) Method

SVMs were originally developed to solve classification problems. However, along with the introduction of Vapnik's ϵ-insensitive loss function [15], they have also been extended and widely used to solve nonlinear regression problems. In this thesis, SVR methods were developed to provide plant operators with valuable information on the break size of LOCAs so that they can successfully manage a LOCA accident. The prediction of continuous variables is known as regression.

The SVR method is given N training data $\{(\boldsymbol{x}_i, y_i)\}_{i=1}^{N} \in R^m \times R$ where $\boldsymbol{x}_i$ is the input vector to the SVR method and y_i is the actual output value, from which it learns the input-output relationship. The SVR method can be expressed as follow [16]:

$$y = f(\boldsymbol{x}) = \sum_{i=1}^{N} w_i \phi_i(\boldsymbol{x}) + b = \boldsymbol{w}^T \boldsymbol{\phi}(\boldsymbol{x}) + b \tag{12}$$

where the function $\phi_i(\boldsymbol{x})$ is called the feature that is non-linearly mapped from the input space $\boldsymbol{x}$, $\boldsymbol{w} = [w_1\ w_2\ \cdots\ w_N]^T$, and $\boldsymbol{\phi} = [\phi_1\ \phi_2\ \cdots\ \phi_N]^T$.

Eq. (12) is a nonlinear regression model because the resulting hyper-surface is a nonlinear surface hanging over the m-dimensional input space. However, after the input vectors $\boldsymbol{x}$ are mapped into vectors $\boldsymbol{\phi}(\boldsymbol{x})$ of a high dimensional kernel-induced feature space, the nonlinear regression model is turned into a linear regression model in this feature space. The nonlinear function is learned by a linear learning machine where the learning algorithm minimizes a convex functional. The convex functional is expressed as the following regularized risk function, and the parameters $\boldsymbol{w}$ and b are a support vector weight and a bias that are calculated by minimizing the risk function:

$$R(\boldsymbol{w}) = \frac{1}{2}\boldsymbol{w}^T \boldsymbol{w} + \lambda \sum_{i=1}^{N} |y_i - f(\boldsymbol{x})|_\epsilon \tag{13}$$

where

$$|y_i - f(\boldsymbol{x})|_\epsilon = \begin{cases} 0 & |y_i - f(\boldsymbol{x})| < \epsilon \\ |y_i - f(\boldsymbol{x})| - \epsilon & otherwise \end{cases} \tag{14}$$

The constant λ is called a regularization parameter. The regularization parameter determines the trade-off between the approximation error and the weight vector norm. An increase of the regularization parameter λ penalizes larger errors, which leads to a decrease of approximation error. This can also be achieved easily by increasing the weight vector norm. However, an increase in the weight vector norm does not make sure of the good generalization of the SVR model. The constants λ and ϵ are user-specified parameters and $|y_i - f(\boldsymbol{x})|_\epsilon$ is called the ϵ -insensitive loss function [15]. The loss equals zero if the predicted value $f(\boldsymbol{x})$ is within an error level ϵ, and for all other predicted points outside the error level ϵ, the loss is equal to the magnitude of the difference between the predicted value and the error level ϵ (refer to Figs. 9 and 10).

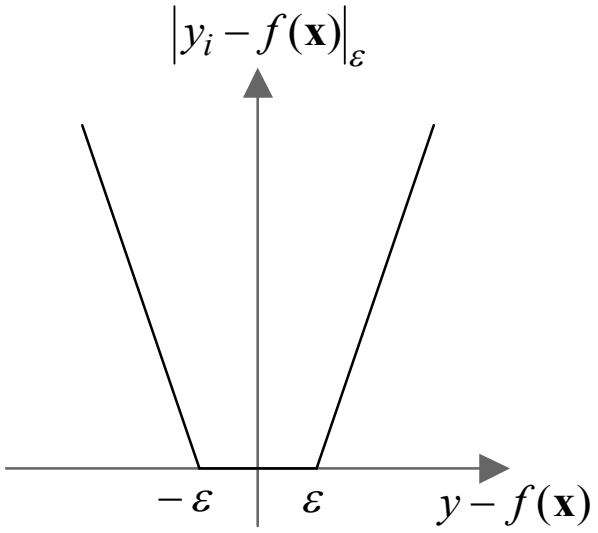

Fig. 9. Linear ϵ-insensitive loss function.

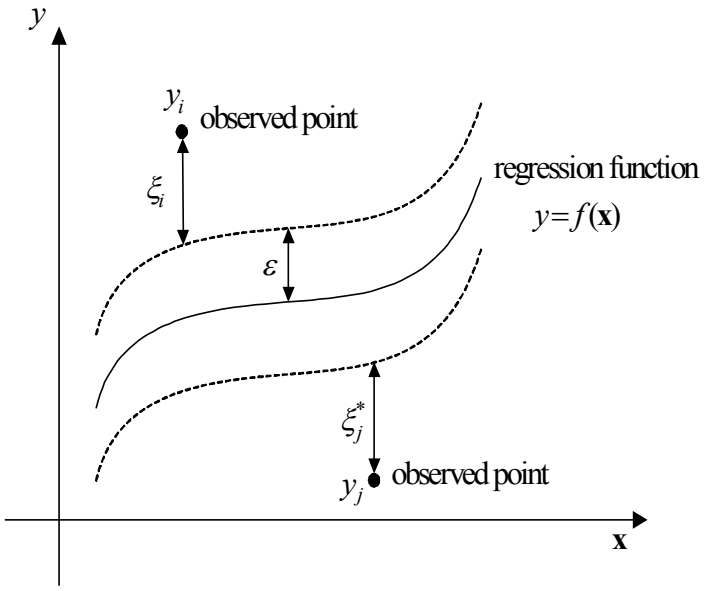

Fig. 10. Insensitive ϵ-tube and slack variables ξ_i and ξ_j^* for the SVR model.

Increasing the insensitivity zone ϵ means a reduction in requirements for the accuracy of approximation and it also decreases the number of support vectors, leading to data compression. In addition, increasing the insensitivity zone ϵ has smoothing effects on modeling highly noisy polluted data. The aforementioned regularized risk function is converted into the following constrained risk function:

$$R(\boldsymbol{w},\xi,\xi^*) = \frac{1}{2}\boldsymbol{w}^T\boldsymbol{w} + \lambda\sum_{i=1}^{N}(\xi_i+\xi_i^*) \tag{15}$$

subject to the constraints

$$\begin{cases} y_i - \boldsymbol{w}^T\boldsymbol{\phi}(\boldsymbol{x}) - b \le \epsilon + \xi_i, & i=1,2,L,N \\ \boldsymbol{w}^T\boldsymbol{\phi}(\boldsymbol{x}) + b - y_i \le \epsilon + \xi_i^*, & i=1,2,L,N \\ \xi_i,\ \xi_i^* \ge 0, & i=1,2,L,N \end{cases} \tag{16}$$

where

$\boldsymbol{\xi} = [\xi_1 \ \ \xi_2 \ \ L \ \ \xi_N]^T$,

$\boldsymbol{\xi}^* = [\xi_1^* \ \ \xi_2^* \ \ L \ \ \xi_N^*]^T$.

The parameter ξ_i and ξ_i^* are slack variables representing upper and lower constraints on the outputs of the system, respectively, and they are positive values (refer to Fig. 10). The constrained optimization problem of (12) can be solved by applying the Lagrange multiplier technique to (12, 13) and then by using a standard quadratic programming technique. Finally, the regression function of (12) becomes

$$y = f(\boldsymbol{x}) = \sum_{i=1}^{N} (\alpha_i - \alpha_i^*) K(\boldsymbol{x}, \boldsymbol{x}_i) + b \tag{17}$$

where $K(\boldsymbol{x}_i, \boldsymbol{x}) = \boldsymbol{\phi}^T(\boldsymbol{x}_i)\boldsymbol{\phi}(\boldsymbol{x})$ is called the kernel function. A number of coefficients $\alpha_i - \alpha_i^*$ have non-zero values and the corresponding training data points are called support vectors (SVs) and have approximation errors equal to or larger than ϵ.

The SVR methods are designed by learning from given data and should be optimized to maximize the prediction performance. The performance of the SVR method depends heavily on the three kinds of design parameters such as an insensitivity zone ϵ, a regularization parameter λ, and a kernel function parameter σ. Therefore, these parameters must be optimized by a genetic algorithm in order to maximize the performance of the SVR model. If these parameters are not optimized, the SVR models can be inferior in performance.

Ⅳ. Application to LOCA Diagnostics

To verify the proposed algorithm, it is essential to acquire the data required to train the SVC, GMDH and SVR models from a number of numerical simulations because there is little real LOCA data. A total of 333 accident simulations were carried out using the MAAP4 code [5] to acquire data, and were composed of 111 hot-leg LOCAs, 111 cold-leg LOCAs and 111 SGTRs.

MAAP4 code has inaccuracy in the simulation results. To assess the inaccuracy, many investigators have made comparisons with other thermal hydraulic codes. Lindholm et al. [17] examined core refloodings using three severe accident analysis computer codes, such as MAAP4, MELCOR, and SCDAP/RELAP5, and reported that all the three codes predicted similar trends in terms of the thermal hydraulic phenomena during the reflood phase. Allison [18] also compared the simulation results of MAAP4 with those of MELCOR and SCDAP/RELAP5 for large break LOCA events. They reported similar results in the early phase even if the user models affected the results in a later phase.

The data used are simulated sensor signals that are acquired from these simulations and consist of a total of 15 signals; core exit temperature, containment pressure and temperature, pressurizer pressure and water level, sump water level, collapsed water level, broken side S/G pressure and temperature, broken side S/G water level, unbroken side S/G pressure and temperature, and unbroken side S/G water level, refueling water storage tank water level, containment mole fraction of H_2. The containment pressure and temperature are measured values at a central position of a containment that is located between the operating deck and the polar crane, which is known as an upper compartment below the dome. APR1400 nuclear power plant has two steam generators. The terms 'broken side S/G' and 'unbroken side S/G' corresponds to the two steam generators that are connected to the broken hot-leg (or cold-leg, SGTs) and the unbroken hot-leg (or cold-leg, SGTs),

respectively. The input variables to the SVC, GMDH, and SVR models are the time-integrated values of 15 simulated sensor signals as follows:

$$x_j = \int_{t_s}^{t_s + \triangle t} g_j(t)dt,\ j = 1, 2, \cdots, 15 \tag{18}$$

where $g_j(t)$ is a specific measured signal, t_s is the scram time and $\triangle t$ is the integrating time span.

In this thesis, since the SVC model is a binary classification model, two SVC models were used to classify three types of events according to their break locations. The two SVC models were trained so that they categorize the hot-leg LOCA, the cold-leg LOCA, and the SGTR as (1, 1), (1, -1), and (-1, -1), respectively as shown in Table 1. The integrating time span in Eq. (18) for the SVC models was 60 sec, which means that the SVC models use the time-integrated signals of a 60 sec time interval immediately after a reactor scram. Among a total of 111 simulations for each break location, the 100 accident simulation data were used to develop the two SVC models and the remaining 11 test datasets were used for an independent verification of the SVC models. In Table 1, the two SVC models classify the break location accurately for the training and test data.

TABLE 1. Identification of the break locations

	Break size (cm^2)	Hot-leg LOCA			Cold-leg LOCA			SGTR			
		Scram time (sec)	Classi-fied		Scram time (sec)	Classi-fied		Break size (cm^2)	Scram time (sec)	Classi-fied	
100 Training simulations	5.07	909.91	1	1	568.91	1	-1	4.50	45.53	-1	-1
	6.13	761.91	1	1	459.91	1	-1	9.00	45.54	-1	-1
	7.30	646.91	1	1	378.91	1	-1	13.49	45.54	-1	-1
	8.56	542.91	1	1	316.91	1	-1	17.99	45.53	-1	-1
	9.93	459.91	1	1	268.91	1	-1	22.49	45.53	-1	-1
	~(90)	~(90)	1	1	~(90)	1	-1	~(90)	~(90)	-1	-1
	681.83	7.63	1	1	6.12	1	-1	481.18	7.67	-1	-1
	693.63	7.60	1	1	6.10	1	-1	485.68	7.60	-1	-1
	705.54	7.50	1	1	6.04	1	-1	490.17	7.54	-1	-1
	717.55	7.42	1	1	5.97	1	-1	494.67	7.50	-1	-1
	729.66	7.34	1	1	5.92	1	-1	499.17	7.44	-1	-1
11 Test simulations	11.40	393.91	1	1	231.91	1	-1	26.98	45.53	-1	-1
	29.19	138.91	1	1	83.63	1	-1	67.46	45.56	-1	-1
	58.58	66.97	1	1	41.63	1	-1	112.43	30.47	-1	-1
	~(5)	~(5)	1	1	~(5)	1	-1	~(5)	~(5)	-1	-1
	447.73	10.13	1	1	7.81	1	-1	382.25	9.54	-1	-1
	548.05	8.80	1	1	6.91	1	-1	427.22	8.56	-1	-1
	658.52	7.84	1	1	6.28	1	-1	472.19	7.79	-1	-1

The GMDH and SVR models did not use all the acquired 15 signals because all the 15 signals has little relationship with LOCA size and also it takes considerable time to train and optimize the GMDH and SVR models if many inputs are used in the GMDH and SVR models. Many measured signals are first screened out from input signals to the GMDH and SVR model by analysis through graphical plotting of input (x-axis) and output (y-axis) signals at many data points and by analyzing

relationship between input and output data through calculating covariance matrix of all acquired data including input and output data. Then additional optimal input selection process was performed by a genetic algorithm. Also, the same 60 sec time integrated values for all input signals were not used and the GMDH and SVR model can have different integrating time of 10 sec to 60 sec (10 sec interval). The integrating time was determined by keeping high the correlation between the specific time-integrated input signal and the output (LOCA break size).

TABLE 2. Input signals and selected input variables for the hot-leg LOCA, cold-leg LOCA, and SGTR

	Input signals	Integrating time (sec)	Selected inputs
Hot-leg LOCA	Core exit temp	10	Containment pressure Pressurizer pressure Pressurizer water level
	Containment pressure	60	
	Containment gas temperature	10	
	Pressurizer pressure	10	
	Pressurizer water level	10	
	Collapsed sump water level	60	
	Collapsed water level	60	
Cold-leg LOCA	Core exit temp	10	Core exit temp Containment gas temperature Collapsed sump water level
	Containment pressure	60	
	Containment gas temperature	30	
	Pressurizer pressure	10	
	Collapsed sump water level	60	
	Collapsed water level	30	
SGTR	Core exit temp	10	Core exit temp Pressurizer water level Broken side S/G water level
	Pressurizer pressure	10	
	Pressurizer water level	10	
	Collapsed water level	50	
	Broken side S/G water level	60	

Among a total of 111 simulations for each break location, the 100 accident simulations were divided into both 50% training simulation data and 20% verification simulation data except for 11 test data. The training data are used to train the GMDH and SVR models and the verification data are used to solve the overfitting problem. The test data is used to independently verify whether or not the GMDH and SVR models work well. Therefore, we used 150 training data (50 hot-leg LOCAs, 50 cold-leg LOCAs, and 50 SGTRs), 60 verification data (20 hot-leg LOCAs, 20 cold-leg LOCAs, and 20 SGTRs), and 33 test data (11 hot-leg LOCAs, 11 cold-leg LOCAs, and 11 SGTRs).

Fig. 11 shows the target and estimated break sizes as well as the relative errors for hot-leg LOCAs using the GMDH models with three input signals (refer to Table 3). Fig. 11(a) shows the target and estimated break sizes for the training data, verification data and test data. In Fig. 11(b), the relative error was and all these errors existed within a bound of 6.8%. Twenty plot points for the verification data and 50 plot points for the training data were connected by a line for easy recognition, and 11 plot points for the test data were also connected by a line. The reason why the relative error is large for small break sizes is because the denominator of the relative error is small. Similar results to Fig. 11 were obtained for the cold-leg LOCA and SGTR, as shown in Figs. 12 and 13.

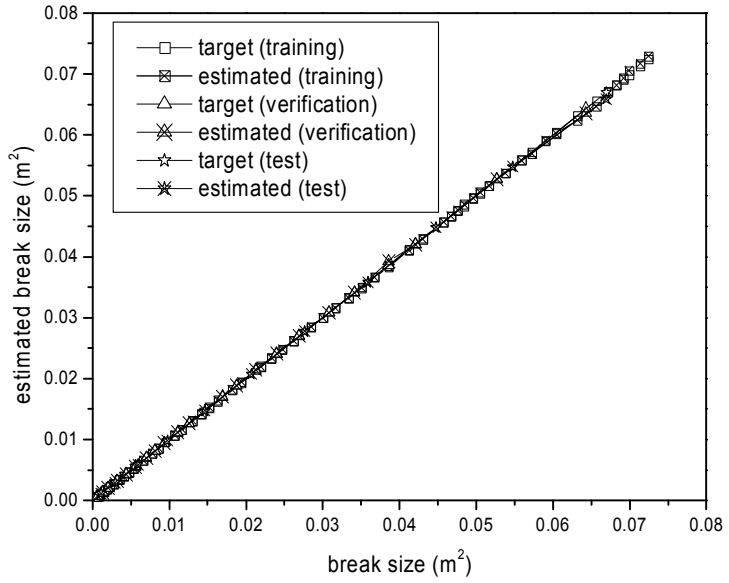

(a) estimated break size

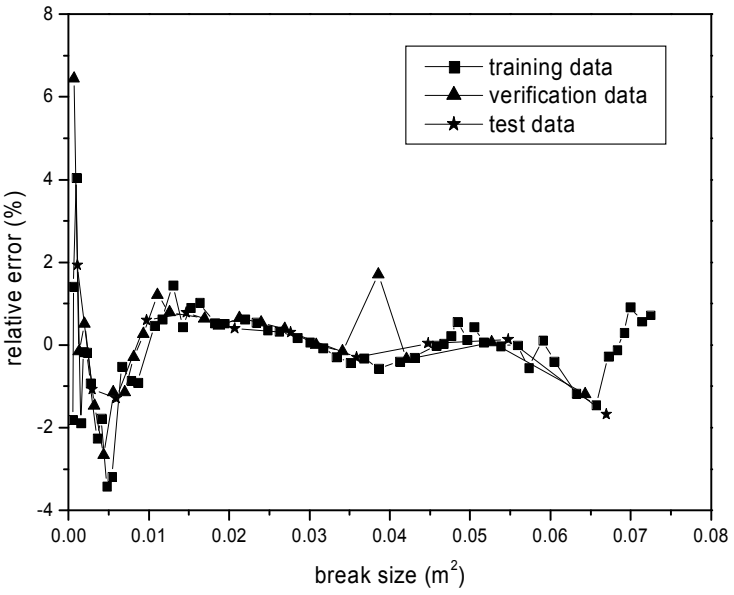

(b) relative error

Fig. 11. Estimated break size and relative errors (hot-leg LOCA)

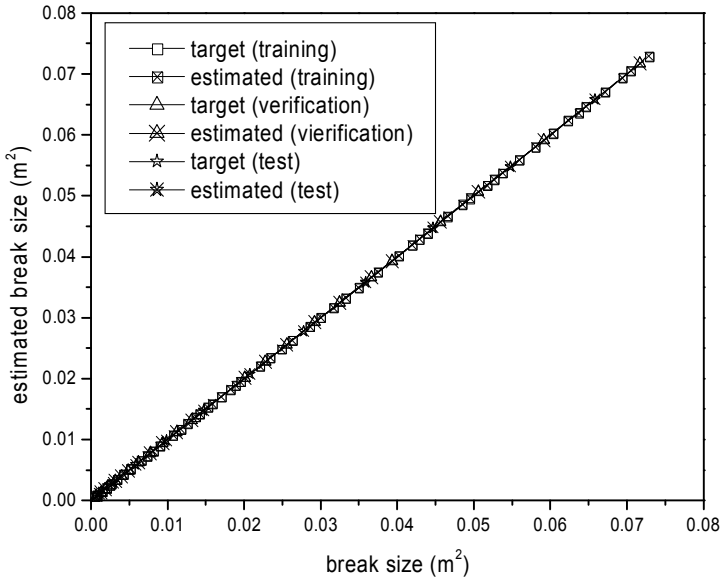

(a) estimated break size

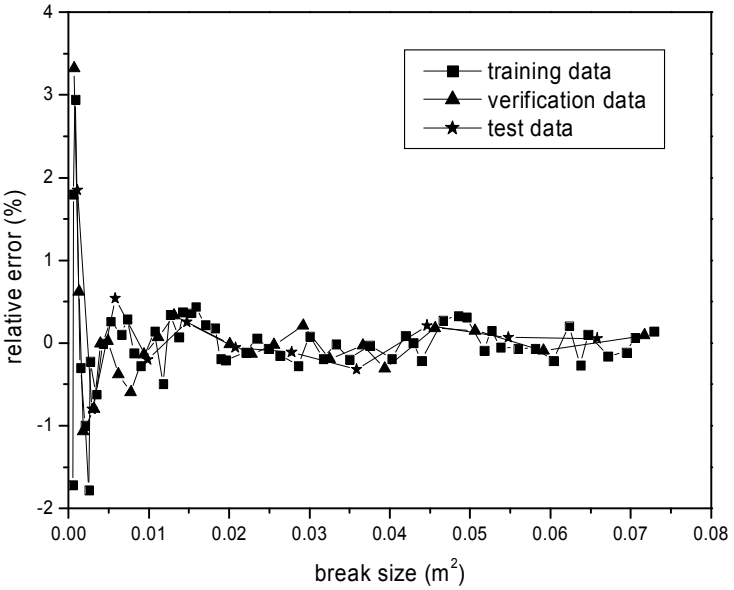

(b) relative error

Fig. 12. Estimated break size and relative errors (cold-leg LOCA)

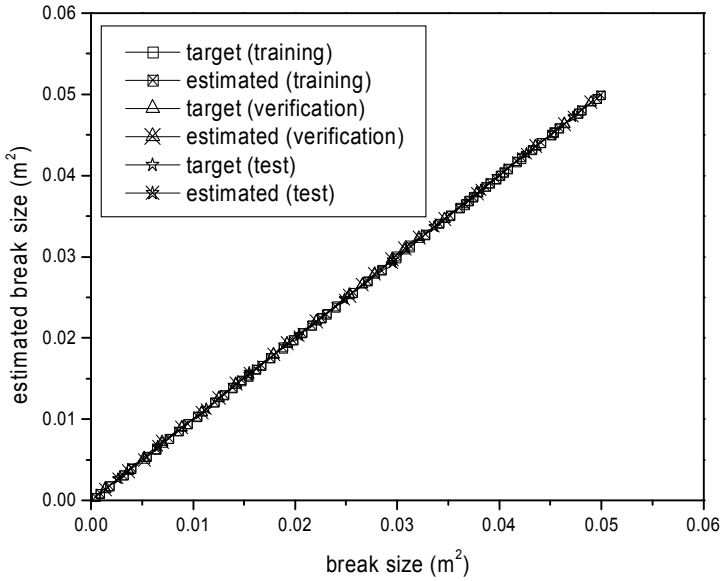

(a) estimated break size

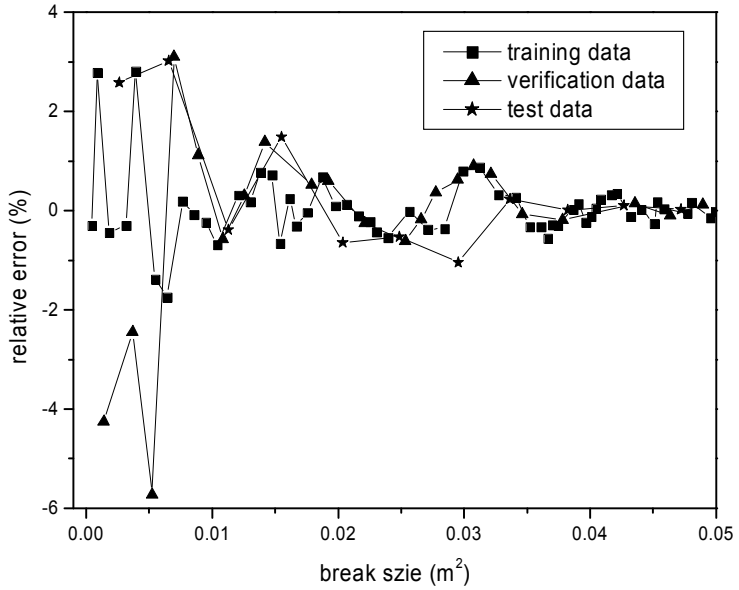

(b) relative error

Fig. 13. Estimated break size and relative errors (SGTR)

Table 3 shows the RMS error of the GMDH models and the SVR models. The number of selected inputs for three types of events is three irrespective of the break locations, respectively. The difference in error between the training data and the test data originates from the size of data because the size of the test data is too small. The difference can be reduced considerably if enough simulation data are provided. As a result of comparison between two models, the GMDH model is superior to the SVR model. A similar study was carried out using the support vector regression (SVR) [4], as shown in Table 4. The RMS errors in the GMDH models were 1.3167%, 0.6820%, and 1.1429% for the hotleg LOCAs, coldleg LOCAs and SGTR, respectively, for the training data, and 0.9862%, 0.6491% and 1.3476% for the test data, as shown in Table 3. In Table 4, the RMS errors for the test data in the SVR models were 1.3776%, 1.0620% and 1.7311% for the hotleg LOCAs, coldleg LOCAs and SGTR, respectively. A comparison between the two models revealed the GMDH model to be superior to the SVR model. The reason why the results of the SVR model are different from the previous result [4] is that more simulation data was used in the present study.

TABLE 3. Estimation errors of the GMDH models

	Selected inputs	Training data (%)		Test data (%)	
		Maximum error	RMS error	Maximum error	RMS error
Hot-leg LOCA	Containment pressure Pressurizer pressure Pressurizer water level	6.4459	1.3167	1.9327	0.9862
Cold-leg LOCA	Core exit temp Containment gas temperature Collapsed sump water level	3.3195	0.6820	1.8511	0.6491
SGTR	Core exit temp Pressurizer water level Broken side S/G water level	5.7249	1.1429	3.0148	1.3476

TABLE 4. Estimation errors of the SVR models

	Selected inputs	Training data (%)		Test data (%)	
		Maximum error	RMS error	Maximum error	RMS error
Hot-leg LOCA	Containment pressure Pressurizer pressure Pressurizer water level	7.4746	1.5446	4.4248	1.3776
Cold-leg LOCA	Core exit temp Containment gas temperature Collapsed sump water level	4.0347	0.9091	2.7938	1.0620
SGTR	Core exit temp Pressurizer water level Broken side S/G water level	6.2021	1.5411	5.2810	1.7311

Since the aforementioned results were generated from simulated data, it was assumed that there were no measurement errors in input signals. In order to analyze the effect of the measurement error on the proposed algorithm, three types of measurement errors are assumed: +5% error, -5% error, and random error. The +5% error option assumes the 5% overmeasurement for all input signals. The random error option assumes that the measurement errors of the input signals have a normal distribution with zero mean and 5% standard deviation. The SVC models discovered break locations without any misclassification despite these measurement errors. Table 5 lists the estimated break size errors by the GMDH models. The RMS errors did not exceed 6% even under these large measurement errors. Although the error magnitude of the GMDH models increases slightly compared to no measurement error, the GMDH models can still accurately estimate the LOCA break sizes. Fig. 14 shows the estimated errors for the hot-leg LOCAs when there are measurement errors. In addition, similar results to Fig. 14 were obtained for the cold-leg LOCAs and SGTR as shown in Fig. 15 and Fig. 16.

TABLE 5. Performance of the GMDH models according to the existence of measurement errors

Error	Hot-leg LOCA			Cold-leg LOCA			SGTR		
	Measurement error			Measurement error			Measurement error		
	+5%	-5%	Random	+5%	-5%	Random	+5%	-5%	Random
RMS Error (%)	5.0214	4.9009	1.9202	5.8077	5.7048	5.6803	5.6236	5.4586	3.9808
Maximum Error (%)	9.6703	9.2759	7.2995	7.3997	6.8841	7.1612	38.5193	34.9322	21.3934

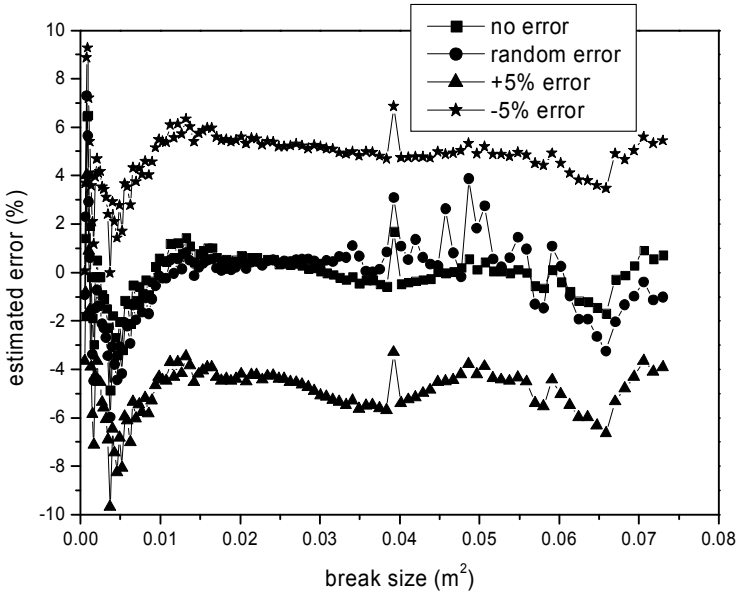

Fig. 14. Estimated errors when measurement errors exist (hot-leg LOCA)

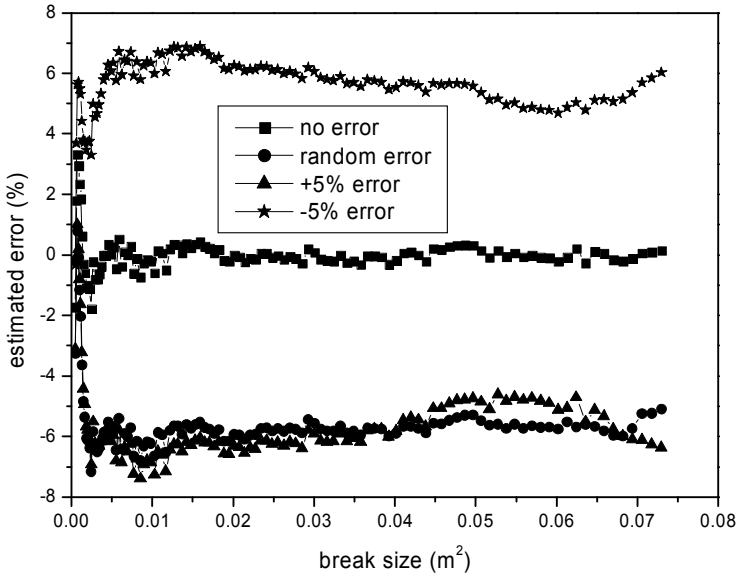

Fig. 15. Estimated errors when measurement errors exist (cold-leg LOCA)

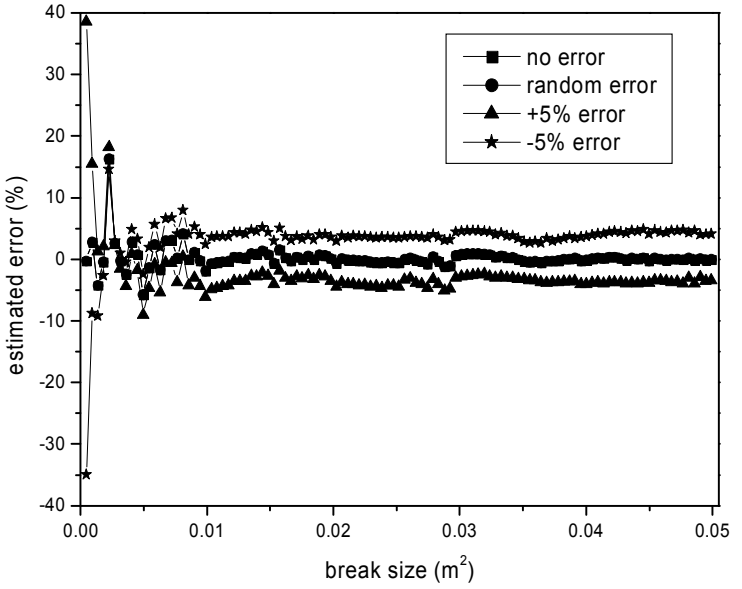

Fig. 16. Estimated errors when measurement errors exist (SGTR)

As the time-integrated signals during a time interval less than or equal to 60 sec after a reactor scram were used for inputs to the SVC and GMDH models, the actuation of the safety systems such as safety injection system (SIS), auxiliary feed water system, and containment spray system, were not considered in this thesis. It is because the initial 60 sec time-integrated signals were used and the safety systems usually start to actuate after a more than 60 sec time delay after the reactor scram. In APR1400 nuclear plants, the time delays of the SIS, the auxiliary feed water system and the containment spray system are 40 sec, 60sec, and 80 sec, respectively. Therefore, the effect of only SIS actuation was investigated because it begins to actuate within a period of 60 second after a reactor scram. The additional simulation data with SIS actuation were used to verify the SVC and GMDH models. The accident simulations with the actuation of the safety systems consist of 5 hot-leg LOCAs, 5 cold-leg LOCAs and 5 SGTRs. Even in this case, the SVC model discovered the break locations without any misclassification and the GMDH models accurately estimate the break sizes. The maximum relative errors of the GMDH models did not exceed 4% for all the accident types (refer to Table 6). Fig. 17 shows the estimated errors for the hot-leg LOCAs in the case where the safety systems actuate. In addition, similar results to Fig 17 were obtained for the cold-leg LOCA and SGTR, as shown in Fig. 18 and Fig. 19.

Given the assumption that the computer code used to acquire the training data accurately describes the phenomena of these accidents within a short time interval after a reactor scram, this method can be applied as a monitoring system in a real nuclear power plant. Fortunately, previous results [17], [18] showed that the accident simulation data is accurate at least in the early accident phase. In addition, the proposed algorithm uses only the initial phase data after a reactor scram. Therefore, the proposed algorithm can be applied to real nuclear power plants, even though it was developed based on numerical simulations.

TABLE 6. Performance of the GMDH models according to SIS actuation

Error	Hot-leg LOCA		Cold-leg LOCA		SGTR	
	Safety system actuation		Safety system actuation		Safety system actuation	
	No	Yes	No	Yes	No	Yes
RMS error (%)	0.9862	1.2184	0.6491	0.1812	1.3476	0.7163
Maximum error (%)	1.9327	1.9593	1.8511	0.3321	3.0148	1.5248

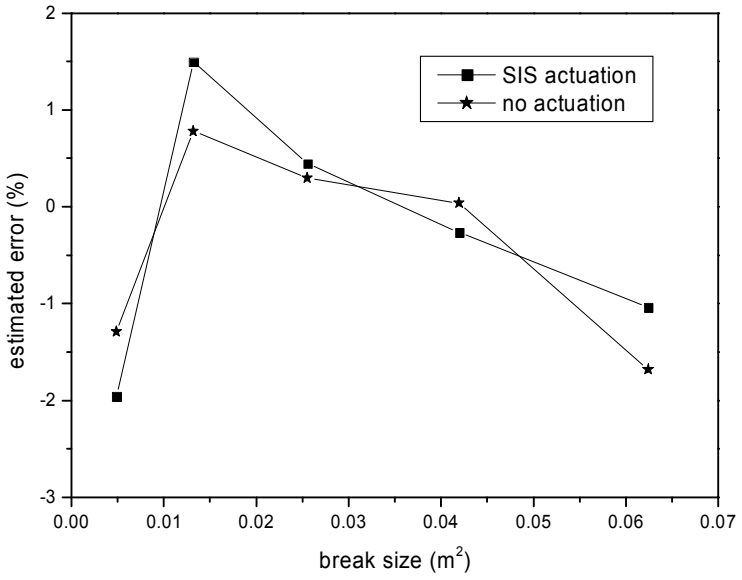

Fig. 17. Estimated errors when the safety systems actuate (hot-leg LOCA)

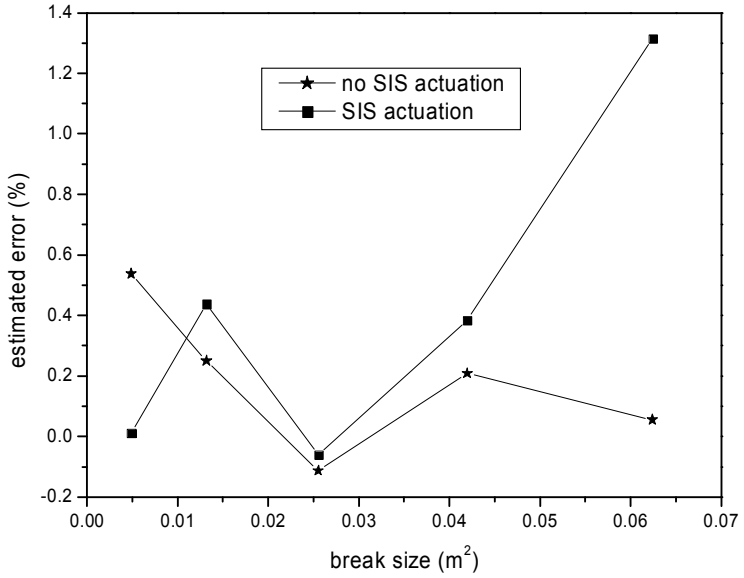

Fig. 18. Estimated errors when the safety systems actuate (cold-leg LOCA)

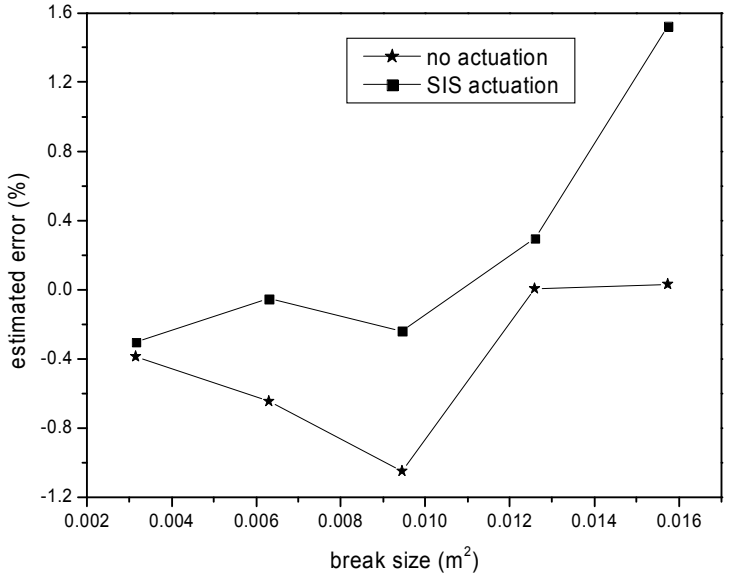

Fig. 19. Estimated errors when the safety systems actuate (SGTR)

Ⅴ. Conclusions

The aim of this thesis was to diagnose loss of coolant accidents (LOCAs) using SVC, GMDH and SVR models. The SVC models were developed to discover the break locations and the GMDH and SVR model was developed to estimate the break size using the 60 sec or less than 60 sec time-integrated signals after a reactor scram. The SVC models were used as a non-linear pattern classifier that identify the major LOCA break locations representing the hot-leg, cold-leg, and steam generator tubes (SGTs) by observing measured signals during a very short time immediately after a reactor scram. The SVC, GMDH and SVR models were trained using the simulation data set (training data) prepared for training and were verified using another simulation data set (test data) independent of the training data. The GMDH and SVR models were also optimized using a genetic algorithm.

The 300 accident simulation data (based on MAAP4) were used to develop the SVC, GMDH and SVR models, and the 33 test data were used to independently verify whether or not the SVC, GMDH and SVR models work well. The simulation results confirm that the proposed SVC model can discover the break location without any misclassification and the proposed GMDH and SVR models can accurately estimate the break size. In addition, in spite of measurement error and safety system actuation, it was shown that the proposed SVC, GMDH and SVR models worked well.

References

[1] S. W. Cheon and S. H. Chang, "Application of neural networks to a connectionist expert system for transient identification in nuclear power plants," Nucl. Technol., vol. 102, no. 2, pp. 177-191, May 1993.

[2] Y. Bartal, J. Lin, and R. E. Uhrig, "Nuclear power plant transient diagnostics using artificial neural networks that allow "don't-know" classifications," Nucl. Technol., vol. 110, no. 3, pp. 436-449, June 1995.

[3] M. G. Na, S. M. Lee, S. H. Shin, D. W. Jung, S. P. Kim, J. H. Jeong, and B. C. Lee, "Prediction of major transient scenarios for severe accidents of nuclear power plants," IEEE Trans. Nucl. Sci., vol. 51, no. 2, pp. 313-321, April 2004.

[4] M. G. Na, W. S. Park, and D. H. Lim, "Detection and diagnostics of loss of coolant accidents using support vector machines," IEEE Trans. Nucl. Sci., vol. 55, no. 1, pp. 628-636, Feb. 2008.

[5] R. E. Henry, et al., MAAP4 - Modular Accident Analysis Program for LWR Power Plants, User's Manual, Fauske and Associates, Inc., vol. 1, 2, 3, and 4, 1990.

[6] T. V. Santosh, A. Srivastava, V.V.S. Sanyasi Rao, A.K. Ghosh, H.S. Kushwaha, "Diagnostic system for identification of accident scenarios in nuclear power plants using artificial neural networks", Reliability Engineering and System Safety, Aug. 2008.

[7] Santosh G. Vind, A.K. Babar, H.S. Kushwaha, V. Venkat Raj, "Symptom based diagnostic system for nuclear power plant operations using artificial neural networks", Reliability Engineering and System Safety, Apr. 2003.

[8] T. V. Santosh, Gopika Vinod, R.K. Saraf, A.K. Ghosh, H.S. Kushwaha, "Application of artificial neural networks to nuclear power plant transient diagnosis", Reliability Engineering and System Safety, Oct. 2007.

[9] Bo-Suk Yang, Won-Woo Hwang, Myung-Han Ko, and Soo-Jong Lee, "Cavitation detection of butterfly valve using support vector machines," J. Sound

and Vibration, vol. 287, nos. 1-2, pp. 25-43, Oct. 2005.
[10] S.J. Farlow, "Self-Organizing Methods in Modeling: GMDH Type Algorithms," Marcel Dekker, New York, 1984.
[11] C.R. Hild, "Development of The Group Method of Data Handling With Information-based Model Evaluation Criteria: A New Approach to Statistical Modeling," Ph.D. Dissertation, The University of Tennessee, Knoxville, August 1998.
[12] P.B. Ferreira and B.R. Upadhyaya, "Incipient Fault Detection and Isolation of Sensors and Field Devices," Research Report, Nuclear Engineering Department, The University of Tennessee, Knoxville, UTNE/BRU/99-02, December 1999.
[13] D. E. Goldberg, Genetic Algorithms in Search, Optimization, and Machine Learning. Reading, Massachusetts: Addison Wesley, 1989.
[14] M. Mitchell, An Introduction to Genetic Algorithms. Cambridge, Massachusetts: MIT Press, 1996.
[15] V. N. Vapnik, Statistical Learning Theory. New York, NY: John Wiley & Sons, 1998.
[16] V. Kecman, 2001. Learning and Soft Computing. MIT Press, Cambridge, Massachusetts.
[17] I. Lindholm, E. Pekkarinen, and H. Sjovall, "Evaluation of reflooding effects on an overheated boiling water reactor core in a small steam-line break accident using MAAP, MELCOR, and SCDAP/RELAP5 computer codes," Nucl. Technol., vol. 112, no. 1, pp. 42-57, 1995.
[18] C. Allison, "Comparison between MAAP, MELCOR and SCDAP/RELAP5," in Proc. of the Workshop on Severe Accident Research in Japan (SARJ-97), Yokohama, Japan, Oct. 6-8, 1998, pp. 396-401.

감사의 글

지난 2년 동안 집에 있는 시간보다 더 많은 시간을 보낸 I&C Lab... 그동안 신경도 쓰지 못했던 서버의 팬소리와 워크스테이션 돌아가는 소리가 지금 이 순간에는 더욱 크고 정겹게 들립니다. 모든 걸 할 수 있다는 자신감과 열심히 하겠다는 마음을 가지고 2008년의 어느 날 실험실에 들어와서 느꼈던 감정이 가장 먼저 떠오르는 이유는 지난 시간의 후회와 아쉬움, 그리고 앞으로 다가올 미래에 대한 두려움과 설레임 때문이 아닌가 싶습니다. 하지만 지금 느끼고 있는 이러한 감정들이 저를 또 다른 곳에서 움직이게 할 원동력이 되고, 제가 보다 더 발전할 수 있는 밑거름이라고 확신하며 지금 이 순간도 최선을 다 하려고 합니다. 정들었던 이곳에서 지난날의 추억을 회상하며 졸업 논문의 마지막을 작성하고 있는 지금 이 시간을 만들어준 모든 분들에게 감사의 마음을 전합니다.

먼저 실수투성이에 한없이 부족했던 저에게 항상 따뜻한 관심과 세심한 배려를 해주시고, 어느 대학원생과 비교하여도 전혀 손색이 없도록 수많은 경험과 지식뿐만 아니라 사회생활을 불문하고 많은 가르침을 주신 나만균 교수님께 한없는 감사를 드립니다. 또한, 항상 모든 제자들이 잘 되기만을 바라시며 일일이 챙겨주시는 모습과 뜨거운 열정으로 변함없이 학문연구에 매진하시는 모습을 보며 진정으로 사람을 고개 숙일 수 있게 하는 법을 알게 해 주셨습니다. 항상 바쁘신 와중에도 시간을 내시어 상담을 하며 많은 조언을 해주셨던 김숭평 교수님, 학과에 대한 애정이 누구보다도 깊으시고 사석에서도 저의 진로에 대한 관심을 가져주시며 많은 조언을 해주셨던 정운관 교수님, 전공뿐만 아니라 대학원 생활도 작은 사회생활이라면서 많은 것들을 가르쳐 주신 이경진 교수님, 처음으로 교수님이라는 높게만 보였던 벽을 단숨에 허물며 교수님들께 보다 쉽게 다가갈 수 있게 만들어 주신 송종순 교수님, 사석에서 항상 신경을 써 주시며 저를 격려하고 자신감을 북돋아 주실 뿐만 아니라 변함없는 모습으로 연구에 임하시는 김진원 교수님, 모든 교수님들에게 진심으로 머리 숙여 감사드립니다. 그리고 원

자력발전소 현장에 대한 실무적인 강의뿐만 아니라 삶의 이야기도 해주시며 많은 격려를 해주신 이심교 교수님, 늘 바쁘신 와중에도 일주일에 한 번씩 내려오셔서 원자력공학과 학생들을 위해 강의를 해주시는 신원기 교수님, 이기복 교수님께도 진심으로 감사의 말씀을 드립니다.

처음 NICL 실험실에 들어왔을 때 같이 대학원 생활을 하며 희노애락을 함께 했던 저의 정신적인 지주 헌영이형, 인호형, 동혁이형.. 하나라도 더 가르쳐 주려고 하고, 많은 관심과 배려를 해주며 같이 생활했던 1년이라는 시간이 정말 행복했습니다. 처음에는 하나하나 너무 세세하게 관심을 가져 주시고 대학원 막내라고 배려를 해줄 때 부담이 된 게 사실이지만, 지금 생각해보면 그 때의 관심과 배려야말로 지금의 저를 있게 해주었다고 생각합니다. 형들이 졸업하기 전에 직접 말한 적은 없지만 지금에서야 정말 감사하고, 사랑한다는 말을 전하고 싶습니다. 그리고 대학원 생활을 같이 하진 않았지만 학부 때부터 3년이라는 시간을 보내면서 못난 모습을 많이 보였던 저에게 단 한 번도 싫은 소리 안하고, 어떤 상황에서든지 넓은 마음으로 이해해주었던 대섭이 형에게도 정말 감사하다는 말을 전하고 싶습니다. 이렇게 좋은 선배들이 있기 때문에 앞으로 인생을 살면서 닥칠 시련이나 난관들이 두렵지 않을 것 같습니다.

대학원 생활을 하면서 선배들뿐만 아니라 수많은 일을 함께 겪었던 NICL 실험실 후배들한테도 고마운 마음뿐입니다. 항상 짜증내고 화내도 다 받아줄 뿐만 아니라 자기 일은 스스로 어떻게든 끝내려던 모습을 보면서 후배이지만 존경심이 들었던 실험실 2인자 동수, 실험실 생활도 힘든데 사이클로트론 업무까지 하는 모습을 보며 안쓰러운 마음도 들고 많이 도와주지 못해 항상 미안한 마음을 갖게 하는 심원이, 앞으로 들어올 막내들을 데리고 실험실을 책임질 차기 실장 영규, 비록 다른 실험실에 있지만 항상 우리 실험실원 같이 느껴지고 옆에 있으면 든든한 민수, 항상 보면 징징대고 자신의 일을 다른 사람에게 친절(?)하게 나눌 줄 아는 학과실 조교 이민서, 모두 후배들이지만 너희들한테 배운 것도 많고 항상 잘 따라줘서 너무 고맙다. 그리고 실험실을 꽉

차게 해 준 막내들 주현이와 순호.. 너희들이 있어서 실험실이 보다 깨끗해졌고 활기차졌다. 다음 학기에 대학원에 진학하게 될 주현이는 앞으로 실험실 선배들 말 잘 따르며 열심히 생활하길 바라고, 순호는 NtUss 논문을 잘 마무리하고 정식으로 대학원에 입학해서 뜻 깊은 시간을 보내길 바란다.

학과 동아리 꼭되기 활동을 하면서 많은걸 가르쳐주고 좋은 추억을 만들어준 세희형, 용하형, 은필이형, 병국이형, 정현이형, 응서형, 승기형, 준이형, 재욱이형, 승진이형, 준환이형, 은경누나, 종화누나 그리고 2학년에 복학하고 나서 학과 생활을 잘 모를 때 이것저것 알려주면서 많이 도와준 01학번 선배들 구일이형, 영춘이형, 희망이형, 봉주형, 진행이형, 우진이형, 선희형, 종현이형 정말 감사하다는 말을 전하고 싶습니다. 대학원 생활을 하면서 조언도 많이 해주시고 힘들 때 술한잔으로 위로해 주던 유선이형, 정민이형, 대학원이라는 매개체를 통해 알게 되고 좋은 말씀을 많이 해 주신 상준이 형, 정현이형, 용진이형 진심으로 감사합니다. 항상 추석, 설날 때 뵈며 교수님과의 이전 추억을 말씀해 주시고 실제적으로 실험실의 궁금한 점을 해결해 주시는 영록이형, 동원이형, 선호형, 인준이형, 선미 누나 앞으로도 잘 부탁드립니다.

학부 생활을 같이 하며 졸업할 때까지 함께 동고동락한 내 동기들 강일, 오웅, 영만, 요환, 준근, 영빈, 태훈, 항국 그리고 후배들 평규, 재환, 상헌, 석철, 용환, 시곤, 윤화, 수민 등등 같이 있을 때는 한 번도 말하지 못했지만 나를 지탱해 주는 힘이 되어 주어 고마웠다. 자주 보지 못하지만 맡은 일에 최선을 다하며 앞으로도 서로에게 힘이 되어주는 존재가 되자꾸나. 그리고 학번이 깡패라고 싫으나 좋으나 잘 따라준 경훈, 기로, 민영, 사용, 작은 주현, 영국, 혜성, 진옥, 현민, 경준, 창수 등 후배들 너무 고맙다. 항상 친구라는 행복감을 안겨주고 함께 울고 웃으며 15년이라는 시간을 함께해준 친구들 진완, 성택, 성용, 승리, 진선, 병윤, 정희, 건의, 용석, 문석, 명진, 상현, 경웅, 준경이 등등 너무너무 고맙고 앞으로 남은 평생 동안 서로 의지하고 잘 지내보자.

마지막으로 저희 남매를 위해 지금껏 자신을 희생하시며 한없는 사랑을 주신 부모님께 머리 숙여 감사의 말씀을 전합니다. 그간 저희 남매를 키우시면서 수많은 마음고생을 하시면서 묵묵히 지켜봐 주신 부모님의 사랑에 감사하다는 말밖에 드릴 말씀이 없습니다. 앞으로 살아가면서 부모님께 물질적인 것만이 아니라 정신적으로도 항상 뿌듯함과 기쁨을 느끼실 수 있도록 항상 노력하고 자랑스러운 모습을 보여드리겠습니다. 쑥스러움에 단 한 번도 직접 말하지 못했지만 사랑합니다. 그리고 사랑하는 동생 혜련이.. 나보다 먼저 졸업하고 취직해서 부모님을 챙기는 모습을 보며 오빠로서 정말 뿌듯하고 자랑스럽다. 그동안 조용히 오빠를 많이 챙겨줘서 고맙고, 항상 좋은 일만 가득하길 바란다.

수많은 추억을 담고 있는 NICL 실험실을 이젠 후배들에게 맡기고 가벼운 마음으로 사회로의 첫발을 내딛으려 합니다. 사회에 첫발을 내딛게 될 두려움과 설렘, 그리고 많은 분들에 대한 고마움 등 만감이 교차하는 지금 이 순간을 뒤로하며..

2010년 12월

NICL실험실에서

이 성 한

저작물 이용 허락서

학 과	원자력공학과	학 번	20097084	과 정	석사
성 명	한글: 이 성 한 한문 : 李 成 漢 영문 : Lee Sung-Han				
주 소	광주광역시 북구 우산동 3-23				
연락처	E-MAIL : sunghan2da@naver.com				
논문제목	한글 : 인공지능 방법을 이용한 LOCA 진단에 관한 연구				
	영문 : A Study on LOCA Diagnostics Using Artificial Intelligence Methods				

본인이 저작한 위의 저작물에 대하여 다음과 같은 조건아래 조선대학교가 저작물을 이용할 수 있도록 허락하고 동의합니다.

- 다 음 -

1. 저작물의 DB구축 및 인터넷을 포함한 정보통신망에의 공개를 위한 저작물의 복제, 기억장치에의 저장, 전송 등을 허락함
2. 위의 목적을 위하여 필요한 범위 내에서의 편집·형식상의 변경을 허락함. 다만, 저작물의 내용변경은 금지함.
3. 배포·전송된 저작물의 영리적 목적을 위한 복제, 저장, 전송 등은 금지함.
4. 저작물에 대한 이용기간은 5년으로 하고, 기간종료 3개월 이내에 별도의 의사 표시가 없을 경우에는 저작물의 이용기간을 계속 연장함.
5. 해당 저작물의 저작권을 타인에게 양도하거나 또는 출판을 허락을 하였을 경우에는 1개월 이내에 대학에 이를 통보함.
6. 조선대학교는 저작물의 이용허락 이후 해당 저작물로 인하여 발생하는 타인에 의한 권리 침해에 대하여 일체의 법적 책임을 지지 않음
7. 소속대학의 협정기관에 저작물의 제공 및 인터넷 등 정보통신망을 이용한 저작물의 전송·출력을 허락함.

동의여부 : 동의(○) 반대( )

2011년 2월 일

저작자: 이 성 한 (서명 또는 인)

조선대학교 총장 귀하